The Reactivation of Tabun-inhibited mutant AChE with Ortho-7: Steered Molecular Dynamics and Quantum Chemical Studies

Journal:	*Molecular BioSystems*
Manuscript ID	MB-ART-11-2015-000735.R1
Article Type:	Paper
Date Submitted by the Author:	21-Jan-2016
Complete List of Authors:	Lo, Rabindranath; CSIR-CSMCRI, Analytical Division and Centralized Instrument Facility Chandar, Nellore; CSIR-CSMCRI, Analytical Division and Centralized Instrument Facility Ghosh, Shibaji; CSIR-CSMCRI, Analytical Division and Centralized Instrument Facility Ganguly, Bishwajit; CSIR-CSMCRI, Analytical Science Division

Journal Name

ARTICLE

The Reactivation of Tabun-inhibited mutant AChE with Ortho-7: Steered Molecular Dynamics and Quantum Chemical Studies

Received 00th January 20xx,
Accepted 00th January 20xx

DOI: 10.1039/x0xx00000x

www.rsc.org/

Rabindranath Lo,[a] Nellore Bhanu Chandar [a,b], Shibaji Ghosh,[a,b] and Bishwajit Ganguly [a,b]

A highly toxic nerve agent, tabun, can inhibit acetylcholinesterase (AChE) at cholinergic sites, which leads to serious cardiovascular complications, respiratory compromise and death. We have examined the structural features of tabun-conjugated AChE complex with an oxime reactivator, Ortho-7, to provide a strategy for designing new and efficient reactivators. The mutated *m*AChE within the choline binding site by (Y337A) and (F338A) with Ortho-7 has been investigated using steered molecular dynamics (SMD) and quantum chemical methods. The overall study shows that after mutagenesis (Y337A), the reactivator can approach more freely towards the phosphorylated active site of serine without any significant steric hindrance in presence of tabun compared to the wild type and double mutant. Further, the poor binding of Ortho-7 with the peripheral residues of *m*AChE in the case of single mutant than that of wild-type and double mutants (Y337A/F338A) can contribute for better efficacy in the former case. Ortho-7 has formed more number of hydrogen bonds with the active site surrounding residues His447 and Phe295 in the case of single mutant (Y337A), and that stabilizes the drug molecule for effective reactivation process. The DFT M05-2X/6-31+G(d) level of theory shows that the binding energy of Ortho-7 with single mutant (Y337A) is energetically more preferred (-19.8 kcal/mol) than the wild-type (-8.1 kcal/mol) and double mutants (Y337A/F338A) (-16.0 kcal/mol). The study reveals that both the orientation of the oxime reactivator for the nucleophilic attack and the stabilization of the reactivator at the active site would be crucial for the design of an efficient reactivator.

Introduction

Organophosphorus compounds (OPs), potent inhibitors of acetylcholinesterase (AChE; EC 3.1.1.7) and butyrylcholinesterase (BChE; EC 3.1.1.8), involve the inhibition processes by phosphylating a serine residue, the active center of the enzyme with the formation of a stable conjugate.[1,2] Such inhibition process disrupts the role of cholinesterase in the termination of nerve impulse transmission at cholinergic synapses, expedite to nervous and respiratory failures.[2] OPs include various pesticides (paraoxon, parathion, tetraethyl pyrophosphate) and highly toxic nerve agents (sarin, soman, cyclosarin, tabun, methylphosphonothioate). However, the acute toxicity of organophosphorus compounds depends on their class and on drug administration.[3,4] Therefore, it is very challenging to control the propagation of the nerve agents as these compounds are easily synthesized.[5] Over the years, such nerve agents have provided a continual risk to the general public, including the terrorist attack in the Tokyo subway in 1995, the bombing of Kurd civilians during the Iraq–Iran War in 1988, and the bombing of the civilians in Syria on August 21, 2013. In addition to that, various OPs are still utilized as pest-control agents, which results in about 3,000,000 acute intoxications per year, 200,000 of which lead to death.[6,7] Therefore, great effort has been devoted to the neutralization of OP poisoning for the protection of civilians and military populations.[8]

Currently, the therapeutic treatment focuses on the reactivation of the inhibited AChE by using anticholinergic atropine, various types of oximes (pralidoxime, trimedoxime, obidoxime, HI-6, HLö-7) and an anticonvulsant (diazepam).[8,9] Various mono- and bispyridinium oximes are utilized as potent reactivators that can reactivate OP-inhibited AChE. The efficacies of oximes are primarily attributed to the effective binding of the pyridinium ring in the active-site gorge and the suitable orientation of the oxime group for the nucleophilic displacement of conjugated organophosphates.[8] However, the efficiency of the reactivators changes with the structure of the bound organophosphates, the type of enzyme and the oxime.[10]

The crystal structures of AChE[11-15] provide valuable information on the admission of the reactivator to the narrow confines of the active site of an enzyme and the steric restraints generated within the active-site gorge which steer the selectivity in organophosphate inhibition[16] and oxime reactivation.[17] The active site of the enzyme is situated at the

[a] Computation and Simulation Unit (Analytical Division and Centralized Instrument Facility), CSIR-Central Salt & Marine Chemicals Research Institute, Bhavnagar, Gujarat, India-364 002. Fax: (+91)-278-2567562, Telephone: +91-278-2567760 Ext: 6770.E-mail: ganguly@csmcri.org.
[b] Academy of Scientific and Innovative Research, CSIR-CSMCRI, Bhavnagar, Gujarat, India-364 002.

†Electronic Supplementary Information (ESI) available: [Cartesian coordinates of the geometries are given]. See DOI: 10.1039/x0xx00000x

base of a narrow and 18–20-Å deep gorge. Various aromatic residues are along the line of the gorge wall of AChE to form a well-described acyl pocket and choline binding site at the base of the gorge.[18] Therefore, the arrangement of the aromatic residues around the incoming reactivator within the narrow confines of the gorge is considered to be important for the reactivation process.

A new approach has recently been used for the reactivation process with reactivators by employing an enzyme scavenger which can neutralize OP compounds promptly before it approaches the targeted synaptic AChE.[19-21] The OP compounds can thus be catalytically hydrolyzed by a combination of oxime AChE in the plasma space before they reach the tissue.[22] In this respect, the study has been aimed at reactivating the OP-inhibited AChE through a systematic modification of the structures of inhibitors, reactivators and enzyme. In addition, the mutant enzyme (*m*AChE) modified within the choline binding site (Y337A) and the acyl pocket (F295L, F297I) can act as a pseudo-catalytic scavenger for the degradation of OP compounds in conjunction with various oximes.[20]

Recently, the importance of site-directed mutagenesis technology has been realized by changing single or multiple amino acids in various region of AChE for the inhibition of AChE with OPs as well as aging and reactivation processes. By introducing the double mutant F295L/Y337A in cycloheptyl methylphosphonyl thiocholine inhibited AChE, the rate of reactivation was enhanced with oxime reactivator HI-6.[10] In fact, Hu AChE double mutant Y337A/F338A does not show aging when it is inhibited by organophosphorus compounds such as soman, sarin and VX.[21a,b] Furthermore, Kovarik and coworkers reported that there is an enhancement in the reactivation rate with single mutation Y337A and imidazole-containing aldoximes.[21c]

In this article, we have examined the structural features for the reactivation process of tabun-inhibited *m*AChE with the oxime reactivator Ortho-7. Tabun poisoning is a major concern due to its greater toxicity, which leads to death. The reason behind such toxicity of tabun is the greater resistance towards most of the reactivators in the reactivation process. Among many oxime reactivators, Ortho-7 can reactivate the tabun-inhibited mouse AChE (*m*AChE) with an efficiency of 24%.[23] Crystallographic studies suggest that a significant structural orientation occurs in tabun-conjugated *m*AChE as compared to that of *apo-m*AChE.[14] The side-chain conformation of Phe338 in *m*AChE-tabun.Ortho-7 is notably different from the oxime-free active site of tabun-inhibited *m*AChE, whereas the conformation of His447 has been found to be similar to the tabun-conjugated *m*AChE. Such results indicate that the steric hindrance created by Tyr337 and Phe338 can play a crucial role for the reactivation process by an incoming reactivator.[14] In this study, we have modified *m*AChE within the choline binding site (Y337A), (F338A) in various mutation combinations and studied the structural features in the light of steered molecular dynamics and quantum mechanics methods.

Computational Methodology

The PDB structure of the tabun-conjugated *m*AChE protein complexed with Ortho-7 (PDB code: 2JF0) has been chosen from the Protein Data Bank for this study.[14] In this *m*AChE-tabun.Ortho-7 crystal structure, the phosphonyl oxygen atom is seen to be interacting strongly with oxyanion hole (Gly121, Gly122 and Ala204) and the dimethylamine moiety is placed in the acyl-binding pocket of Phe295, Phe297, and Phe338. Furthermore, the ethoxy group located towards the indole ring of Trp86.[14] Such conformation of the tabun-adduct in the active-site is most common and can be seen in non-aged and aged tabun-inhibited AChE.

The AChE enzyme was modified in its choline binding site of the active gorge by replacing the aromatic residues Tyr337 and Phe338 with the aliphatic one (Alanine). The mutation of the enzyme was performed in the Modeler program.[24] Finally, the drug–protein complexes were taken for hydrogen treatment and minimization in the Macromodel program.[25] The GROMACS 4.6.3 software package was taken for simulation study using GROMOS 96 force field.[26] The repaired protein–drug crystal structures were used in this simulation study. After mutation, we took three sets of *m*AChE-drug complexes: mAChE-wild-type, *m*AChE-Y337A, and *m*AChE-Y337A/F338A. All these complexes were initially dipped in the cuboid box filled with water molecules with a distance of 10Å away from the box wall. For the *m*AChE-wild-type:Ortho7 complex, the cubic box was filled with 30154 water molecules and the cubic boxes of *m*AChE-Y337A:Ortho7, and *m*AChE-Y337A/F338A:Ortho7 were filled with 35518, and 30157 water molecules, respectively. For the energy minimization of protein–drug complexes, a flexible SPC water model was utilized with the steepest descent minimization technique. The linear constraint solver algorithm was adopted to constrain the bond lengths with a simulation time step of 2 fs for the integration of the equation of motion for all atoms. Electrostatic interactions were taken into account by using the Particle-Mesh Ewald algorithm with a distance cut-off of 12Å.[27] Both the solvent and solute were separately heated to temperature reservoirs of 300K using the V-rescale temperature coupling method with coupling times of 0.1 ps. Pressure was considered with the Berendsen coupling method with coupling times of 2 ps. A conventional molecular dynamics simulation was carried out for the protein–drug complexes containing the drug, protein, water and ions within 1-ns simulation time.

Further, we have extended our study by an SMD simulation study with the stabilized structures obtained from the conventional molecular dynamics (CMD) method. The SMD simulations demonstrate the exit of the drug molecules from the active-site gorge of *m*AChE with the application of an external time-dependent harmonic force in the z-direction, which is supposed to be the favourable exit route from the gorge.[28-29] We have performed a simulation study of the protein-drug complexes within 5-ns simulation time. We have used the umbrella pulling method for the simulation study under the identical simulation conditions when force constant

= 1686.747 kJ/mol/nm^2 and velocity = 0.0005 nm/ps. In earlier research, this spring stiffness value and pulling velocity were taken for the SMD simulation of a protein–drug complex.[28-29] The pulling force is applied on the center of mass of the Ortho-7 molecule. The results from the SMD-simulation study have been analysed considering the protein–drug rupture-force profile, hydrogen bonding, and hydrophobic interactions using GROMACS[26] and LIGPLOT[30] programs.

Tabun-inhibited wild-type and mutant *m*AChE geometries were taken from the starting complex structures used in SMD simulations and energies were calculated at the M05-2X/6-31+G* level of theory.[31] The phosphorylated active-site serine (SUN203), Ortho-7 and important residues such as (His447, Tyr337, Phe338. Trp86, Tyr72, Trp286, Glu202, Phe295) in the active and peripheral anionic sites were taken for the quantum chemical energy calculations without any capping at N or C terminals. The binding energy is calculated using the following equation,

$$BE = (E_{complex}) - (E_{protein} + E_{drug})$$

All calculations were performed with the Gaussian 09 suite program.[32]

Results and Discussion

We have performed SMD studies for three sets of *m*AChE.Ortho-7 complexes, wild-type, single mutant (Y337A) and double mutants (Y337A/F338A) *m*AChE. Such information would be useful in predicting the binding of Ortho-7 with proteins in terms of hydrogen bonding, different types of drug–protein non-bonded interactions, hydrophobic interactions, the structure and orientation of the drug with various protein residues.[28,29] Therefore, SMD studies will provide insight into the relative contributions of various interactions arising in protein–drug complexes, where the same drug interacts with various proteins of different skeletal structures in the active site. Steered molecular dynamics closely imitator the force application that occur in an atomic force microscopy (AFM) experiment and delivers detail information about the dissociation of a single molecule from the protein environment though pulling experiment.[33-35] We have performed the time-dependent topographical descriptions of three sets of protein–drug complexes for the unbinding process of Ortho-7. A harmonic potential has been applied to pull out the reactivator from the active-site gorge. A relatively low-velocity SMD simulation has been carried out to avoid errors and to deal with the dynamical nature of drug unbinding.

The calculated center-of-mass (COM) separations between the Ortho-7 and OP-inhibited enzymes (wild-type and mutant ones) are given in Fig. S1, ESI. The unbinding process of the drug can easily be seen from the plots of COM separation between the drug and the enzyme (Fig. S1, ESI). It has been reported that to design an efficient reactivator, the nucleophilic part of the reactivator should approach the OP conjugate AChE without facing a larger degree of steric hindrance at the active site.[14] The SMD studies offer the force profiles when Ortho-7 exits from the gorge in the case of wild type, single mutant (Y337A) and double mutant (Y337A/F338A) (Fig. S2, ESI). The force profiles reveal that the single mutant requires larger force to pull the drug molecule from the active site of the enzyme at lower time scales (0-1000 ps) compared to the wild-type and double mutant. During this time frame the drug molecule is residing in the active site while pulling the drug. The force profiles are however, higher at longer time scales in wild type and double mutant (Fig. S2, ESI).

Now, for the nucleophilic attack, the appropriate orientation of ortho-positioned oxime is required towards the electrophilic phosphorus atom conjugated to the active serine (SUN203) of the OP-inhibited AChE. Therefore, we have examined the orientation of Ortho-7 at the time of egress of the reactivator from the active-site gorge by calculating the COM distances between SUN203 and hydroxyl oxygen of the active ring in Ortho-7 (Fig. 1). The plot suggests the orientation of oximate oxygen atoms towards SUN203, which determines the efficiency of reactivator towards the nucleophilic attack on the OP-inhibited enzyme.

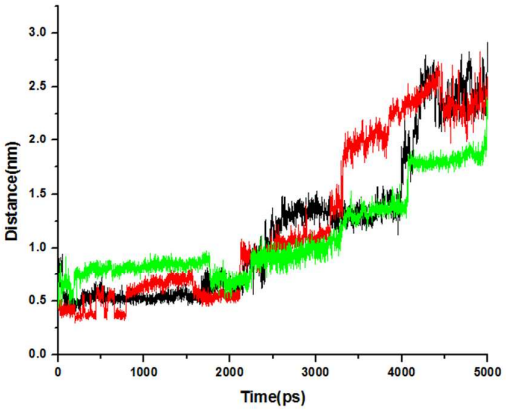

Fig. 1. COM distance plots between SUN203 and oxime oxygen of Ortho-7 for all mutants and wild-type. (Wild-type=black, Y337A=Red, double mutants (Y337A/F338A)=Green)

We have examined the plots for the movement of Ortho-7 with the wild-type, single mutant (Y337A) and the double mutants (Y337A/F338A) *m*AChE (Fig. 1). The COM plot reveals that the drug active oxime oxygen is relatively closer to SUN203 (~3.0 Å) in single mutant (Y337A) compared to the wild-type (~4.0 Å) and double mutants (Y337A/F338A) (~4.4 Å) *m*AChE. The approach of the oxime oxygen of Ortho-7 to the SUN203 is maintained upto ~1000ps in single mutant (Y337A) *m*AChE (Fig. 1).

The examined plots of COM between SUN203 and Ortho-7 have been further substantiated with the temporal spatial distances during the SMD simulations between the center of mass of active-site SUN203 and the N atom of the active pyridinium ring of Ortho-7 (Fig. 2). These plots further suggest that Ortho-7 can reside much closer to the SUN203 in the case of single mutant (Y337A) upto ~1700ps.

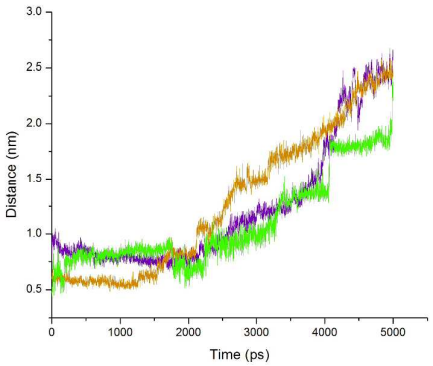

Fig. 2. COM distance plots between active-site SUN203 and the N1 atom of the pyridinium ring of Ortho7 which was initially close to active triad of *m*AChE for mutants and wild-type. (Wild-type=violet, Y337A= dark yellow, double mutants (Y337A/F338A)= Green)

The ability of Ortho-7 to reactivate tabun conjugated AChE has been experimentally studied and compared with some other drugs like HI-6 and obidoxime.[15] Ortho-7 is clearly a superior antidote to reactivate tabun conjugated AChE than HI-6 and obidoxime. The earlier claims of steric hindrance by Ph338 of enzyme is not critical for the movement of Ortho-7 in tabun conjugated AChE, which however is responsible for the lower activity of HI-6. The crystallographic study of *m*AChE.Ortho-7 further suggests that the relatively loose binding of peripheral pyridinium ring and central heptyl linker allow Ortho-7 for easier movement in the enzyme.[15] Furthermore, the role of single mutant to enhance the reactivation process of another oximate drug HLö-7 with tabun conjugated AChE has been reported.[36] The approach of Ortho-7 to SUN203 with the single mutant (Y337A) using SMD simulations also shows the improvement in the reactivation efficacy of the drug as observed with HLö-7.[21a,36,37]

The pyridinium rings in Ortho-7 possess a net positive charge, hence the interaction of pyridinium rings of Ortho-7 with the amino acid residues is also important for the proper orientation of the drug and to augment the reactivation of the inhibited *m*AChE. We have calculated hydrophobic interactions (HIs) between the drug molecule and the particular amino acid residues with the wild-type, single mutant (Y337A) and double mutants (Y337A/F338A) *m*AChE. The peripheral amino acid residues such as Trp286, Tyr72, Tyr124, and Asp74 showed significantly higher hydrophobic interactions with the wild-type and double mutants (Y337A/F338A) (Table 1). The better efficacy of Ortho-7 compared to HI-6 and obidoxime with tabun conjugated AChE was suggested due to loose binding of peripheral pyridinium ring.[15] To get better insight in the orientation of enzyme bound Ortho-7, we have taken snapshots at different time intervals in the wild as well as mutant enzymes (Fig. 3). The peripheral pyridinium ring of Ortho-7 is sandwiched by the aromatic residues of Tyr72 and Trp286 through cation-π interactions in wild and double mutant enzymes (Fig. 3). Such interaction is maintained at 1000 ps time scale in these ortho-7 complexed wild and double mutant enzymes, although it is missing in single mutant (Y337A) enzyme. The weaker HI interactions of Ortho-7 with peripheral anionic site for single mutant (Y337A) compared to wild-type and double mutant can enhance the reactivation ability with the former case.

Table 1. Total numbers of hydrophobic interactions (HI) formed by the residues with Ortho-7 in wild-type and mutant enzymes (Y337A and Y337A/F338A)

Residues	Wild-type	Y337A	Y337A/F338A
TRP86	225	0	290
TRP286	3091	69	945
TYR72	201	0	265
TYR124	926	40	149
TYR337	274	213	0
TYR341	1290	2076	1972
GLY122	4	0	0
ALA361	0	332	194
ASP74	37	0	3
LEU360	0	81	1
PHE295	311	344	447
PHE338	316	2018	0
HIS447	0	0	0
GLU334	0	147	165
SUN203	313	403	285
PHE297	517	389	340

Wild-type

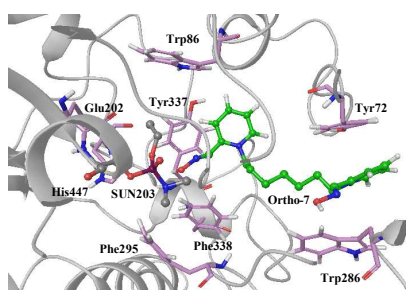

0 ps

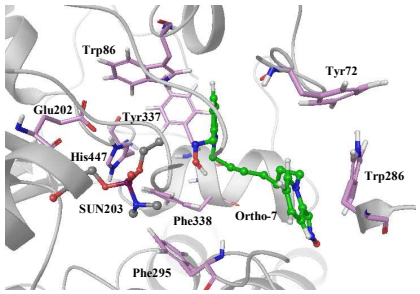

1000 ps

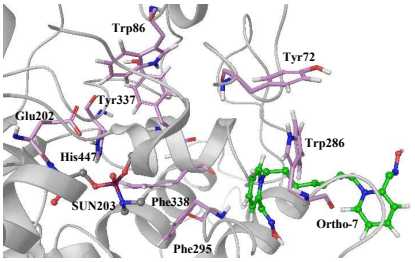

3000 ps

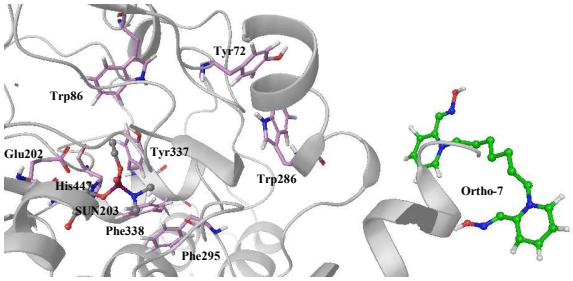

5000 ps

Y337A

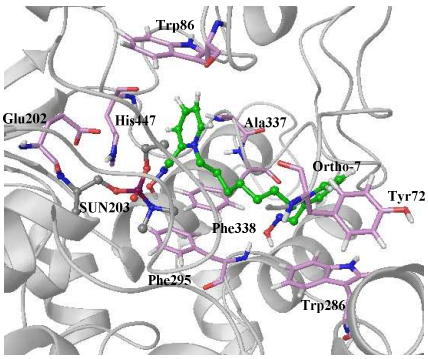

0 ps

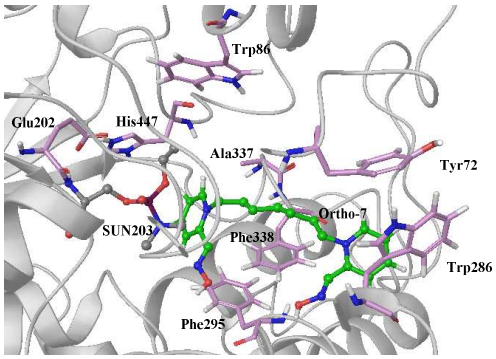

1000 ps

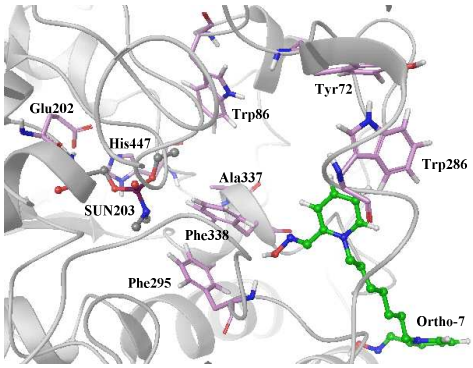

3000 ps

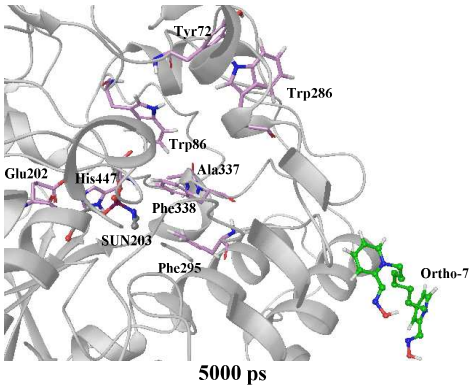

5000 ps

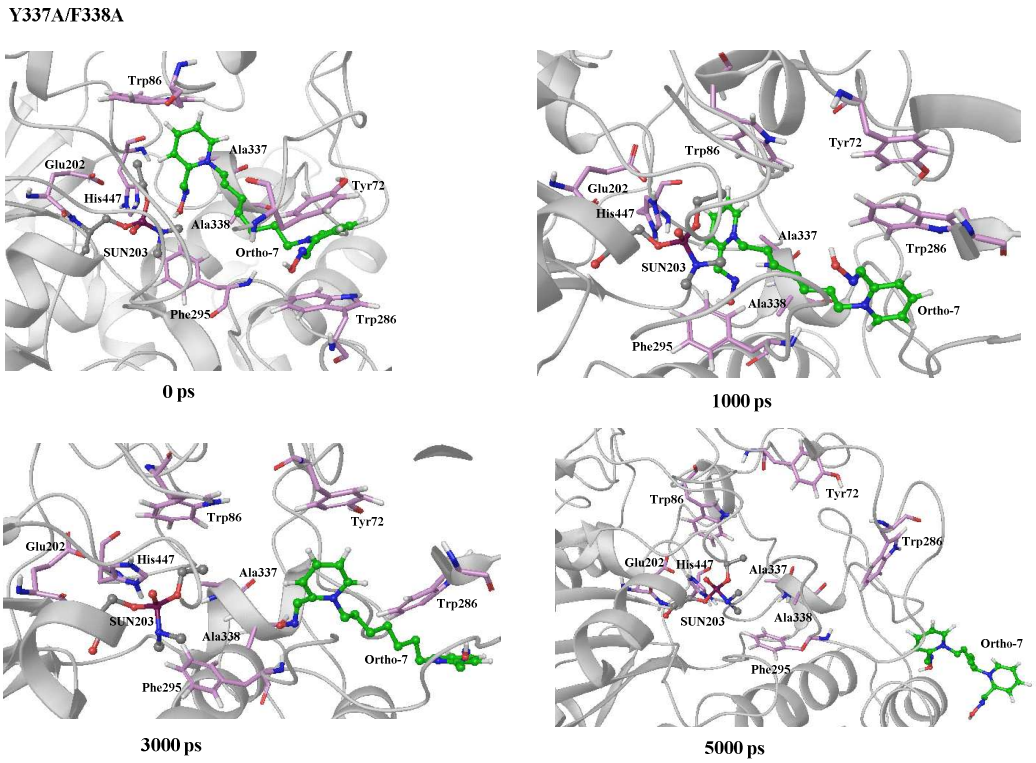

Fig. 3. The pictorial representation of the Ortho-7 inside the active gorge of wild and mutant enzymes (Y337A and Y337A/F338A) at different time scale during the unbinding of Ortho-7 as a function of time from the active site gorge.

It is known that the direct hydrogen-bonding interactions (DHBs) play a significant role in stabilizing the reactivator at the active gorge of the enzyme.[28] The overall hydrogen bonding observed with wild-type, single mutant (Y337A) and double mutants (Y337A/F338A) reveals that there are more number of hydrogen bonds formed with Ortho-7 and single mutant (Y337A) than that of wild-type up to ~2000ps (Fig. 4). From the SMD COM distance plots and snapshots data it is clear that the reactivator is lying closer to the active site gorge up to ~1600ps to ~2000ps and then starts to egress from the active site of enzyme. Therefore, the hydrogen bonding up to ~2000ps will be important to keep the reactivator near to the active site gorge, and the efficacy of reactivator would be dependent for better reactivation process.

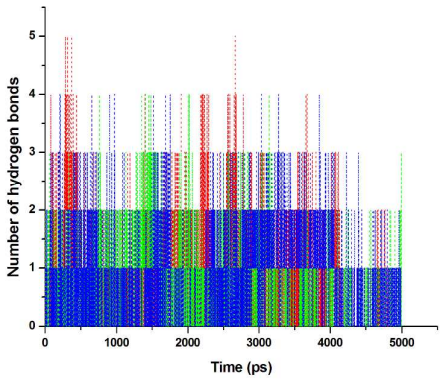

Fig. 4 Temporal evolution of the number of hydrogen bonds formed between Ortho-7 and amino acid residues of wild and mutants *m*AChE. Wild-type=Red, single mutant (Y337A)= Green, Double mutant(Y337A/F338A)= Blue

From the hydrogen bonding data it has been observed that Tyr124 is the only residue which forms numbers of hydrogen bonding with the reactivator up to ~2000ps in the case of wild-type enzyme (Fig. S3, ESI). In the case of single mutant Y337A, SUN203 forms significant numbers of hydrogen bonding with the reactivator within ~2000ps compared to wild-type, and

suggests the closeness of Ortho-7 towards SUN203 of tabun-inhibited AChE. In the case of single mutant Y337A, hydrogen bonds also exist with catalytic triad residue His447, and such interaction was not observed in the wild-type enzyme. The residue Phe295 is located in the active site region, near the SUN203 residue, which also forms more number of hydrogen bonds within ~2000ps in the case of single mutant Y337A than that of wild-type. Residues Arg364, Ala361, Val343, Gly342 and Phe338 are also formed number of hydrogen bonds with the drug molecule in the case of single mutant Y337A. These hydrogen bonding results are also in line with the COM distances and snapshots data as given above (Fig. 1, 3 & S3, ESI). The hydrogen bonding data observed with double mutants (Y337A/F338A) showed somewhat better interaction compared to wild-type with Ala338 and Phe295 during the simulation process (Fig. S3, ESI).

The stabilization of Ortho-7 with single mutant enzyme (Y337A) superior to wild-type and double mutants (Y337A/F338A) has further been examined using quantum chemical calculations. The quantum chemical calculations have been performed with the final geometries of conventional molecular dynamics calculations, the phosphorylated active-site serine (SUN203), Ortho-7 and various important residues at the active site of the enzyme (His447, Tyr337, Phe338, Trp86, Glu202 and Phe295) and peripheral site (Tyr72, Trp286) were considered. The stability of Ortho-7 with modelled active site residues employing M05-2X/6-31+G(d) level of theory shows that the binding energy of Ortho-7 with single mutant (Y337A) is more preferred than the wild-type and double mutant (Y337A/F338A) case (Table 2). M05-2X DFT functional was taken in this study as it accounts for the dispersion interactions more accurately for such non-bonded interactions.[31a] Therefore, these results corroborate that Ortho-7 can function as a better reactivator with single mutant (Y337A) compared to wild-type enzyme and double mutants (Y337A/F338A).

Table 2. The calculated binding energies of Ortho-7 with wild-type and mutant enzymes (Y337A, and Y337A/F338A) at the M05-2X/6-31+G(d) level of theory.

	Binding energy (kcal/mol)
Wild-type	-8.1
Y337A	-19.8
Y337A/F338A	-16.0

Conclusions

This work reports steered molecular dynamics studies for the reactivation of tabun-inhibited *m*AChE with Ortho-7 in wild-type and mutant *m*AChE. In the mutation study, tabun-inhibited *m*AChE has been modified within the choline-binding site with single (Y337A) and double mutants (Y337A/F338A). SMD results showed some interesting trends towards the reactivation process of tabun-inhibited AChE in wild-type and mutant AChE with Ortho-7. The center of mass (COM) analyses suggest that Ortho-7 can approach SUN203 more efficiently with single mutant (Y337A) than the wild-type and double mutants (Y337A/F338A). The drug active oxime oxygen is relatively closer to SUN203 (~3.0 Å) in single mutant (Y337A) compared to the wild-type (~4.0 Å) and double mutants (Y337A/F338A) (~4.4 Å) *m*AChE. Therefore, single mutant (Y337A) *m*AChE gives more conformational flexibility to approach the drug molecule towards the phosphorylated conjugate without facing several steric constraints at the active-site of the enzyme. The approach of Ortho-7 in single mutant (Y337A) is relatively easier due to the poor binding affinity with the peripheral residues of *m*AChE. We have observed that peripheral amino acid residues such as Trp286, Tyr72, Tyr124, and Asp74 of wild-type and double mutants (Y337A/F338A) *m*AChE showed significantly higher hydrophobic interactions with the Ortho-7, whereas for single mutant (Y337A) *m*AChE hydrophobic interactions are relatively lower with Ortho-7. Interestingly, in the case of single mutant (Y337A), Ortho-7 is forming more number of hydrogen bonds with the active site surrounding residues His447 and Phe295 and presumably that can lead to stabilize the drug molecule for effective reactivation process. The quantum chemical calculations performed with DFT M05-2X/6-31+G(d) level of theory shows that the binding energy of Ortho-7 with single mutant (Y337A) is energetically more preferred (-19.8 kcal/mol) than the wild-type (-8.1 kcal/mol) and double mutants (Y337A/F338A) (-16.0 kcal/mol). These QM results are in the line of agreement with the force profiles generated while pulling the drug molecule from the active site gorge of AChE and its mutants. This computational study sheds light on the improved reactivation ability of Ortho-7 towards one of the most resistant OPs i.e., tabun inhibited AChE with mutagenesis and would excite the experimentalists to examine such cases.

Acknowledgements

CSIR-CSMCRI Communication number: 180/2014. One of the authors RL is thankful to UGC, New Delhi, India and NBC is thankful to CSIR, New Delhi, India for awarding senior research fellowship. Shibaji Ghosh is thankful to AcSIR and CSIR-CSMCRI for giving him the opportunity for the doctoral program. We are thankful to Dr. Tusar Bandyopadhyay, Theoretical Chemistry Section, Chemistry Group, Bhabha Atomic Research Centre, Trombay, Mumbai, India for providing the pdb structures of mutant AChEs. BG thanks (MSM, SIP, CSIR, New Delhi) and Department of Atomic Energy-Board of Research in Nuclear Sciences, Mumbai for financial support. We are also thankful to the reviewers for their suggestions and comments that have helped us to improve the paper.

Notes and references

1 W. N. Aldridge and E. Reine, Enzyme inhibitors as substrates. North-Holland, Amsterdam, 1972.

2 P. Taylor, The Pharmacological Basis of Therapeutics, 8th ed. (Gilman AG, Goodman LS, Rall TW and Murad F, Eds.), 1990, 131–149, Macmillan, New York.
3 T. C. Marrs, *Pharmacol. Ther*. 1993, **58**, 51.
4 F. R. Sidell and J. Borak, Annals of Emergency Medicine, 1992, **21**, 865.
5 Convention on the Prohibition of the Development, Production, Stockpiling and Use of Chemical Weapons and on Their Destruction: The Technical Secretariat of the Organization for the Prohibition of *Chemical* Weapons, Den Hague, Netherlands, 1993.
6 M. Eddleston, N. A. Buckley, P. Eyer and A. H. Dawson, *The Lancet*, 2008, **371**, 597.
7 M. Eddleston, L. Karalliedde, N. Buckley, R. Fernando, G. Hutchinson, G. Isbister, F. Konradsen, D. Murray, J. C. Piola, N. Senanayake, R. Sheriff, S. Singh, S. B. Siwach and L. Smit, *The Lancet*, 2002, **360**, 1163.
8 G. Mercey, T. Verdelet, J. Renou, M. Kliachyna, R. Baati, F. Nachon, L. Jean and P. Renard, *Acc. Chem. Res*. 2012, **45**, 756.
9 M. Jokanovića and M. P. Stojiljković, *Eur. J. Pharmacol.* 2006, **553**, 10.
10 Z. Kovarik, Z. Radi, H. A. Berman, V. Simeon-Rudolf, E. Reiner and P. Taylor, *Biochemistry*, 2004, **43**, 3222.
11 J. L. Sussman, M. Harel, F. Frolow, C. Oefner, A. Goldman, L. Toker, I. Silman, *Science*, 1991, **253**, 872.
12 Y. Bourne, P. Taylor, P. Marchot, *Cell*, 1995, **83**, 503.
13 G. Kryger, M. Harel, K. Giles, L. Toker, B. Velan, A. Lazar, C. Kronman, D. Barak, N. Ariel, A. Shafferman, I. Silman and J. L. Sussman, *Acta Crystallogr Sect D* 2000, **56**, 1385.
14 F. J. Ekstrom, C. Astot and Y. P. Pang, *Clin. Pharm. Ther.* 2007, **82**, 282.
15 F. Ekström, Y-P. Pang, M. Boman, E. Artursson, C. Akfur and S. Bérjegren, *Biochem pharm* 2006**, 72**, 597.
16 (a) H. A. Berman and K. Leonard, *J. Biol. Chem.* 1989, **264**, 3942; (b) N. A. Hosea, H. A. Berman and P. Taylor, *Biochemistry*, 1995, **34**, 11528; (c) N. A. Hosea, Z. Radić, I. Tsigelny, H. A. Berman, D. M. Quinn and P. Taylor, *Biochemistry*, 1996, **35**, 10995; (d) P. Taylor, N. A. Hosea, I. Tsigelny, Z. Radić and H. A. Berman, *Enantiomer*, 1997, **2**, 249; (e) A. Ordentlich, D. Barak, C. Kronman, H. P. Benschop, L. P. A. De Jong, N. Ariel, R. Barak, Y. Segall, B. Velan and A. Shafferman, *Biochemistry*, 1999, **38**, 3055; (f) Z. Kovarik, Z. Radić, H. A. Berman, V. Simeon-Rudolf, E. Reiner and P. Taylor, *Biochem. J.* 2003, **373**, 33.
17 (a) Y. Ashani, Z. Radić, I. Tsigelny, D. C. Vellom, N. A. Pickering, D. M. Quinn, B. P. Doctor and P. Taylor, *J. Biol. Chem.* 1995, **270**, 6370; (b) H. Grosfeld, D. Barak, A. Ordentlich, B. Velanand and A. Shafferman, *Mol. Phamacol*. 1996, **50**, 639; (c) P. Masson, M. –T. Froment, C. F. Bartels and O. Lockridge, *Biochem. J.* 1997, **325**, 53; (d) O. Lockridge, R. M. Blong, P. Masson, M. –T. Froment, C. B. Millard and C. A. Broomfield, *Biochemistry*, 1997, **36**, 786; (e) L. Wong, Z. Radić, R. J. M. Brüggemann, N. Hosea, H. A. Berman and P. Taylor, *Biochemistry*, 2000, **39**, 5750.
18 (a) Z. Radić, N. A. Pickering, D. C. Vellom, S. Camp and P. Taylor, *Biochemistry*, 1993, **32**, 12074; (b) A. Ordentlich, D. Baraks, C. Kronman, Y. Flashner, M. Leitner, Y. Segalls, N. Ariel, S. Cohen, B. Velan and A. Shafferman, *J. Biol. Chem.* 1993, **268**, 17083.
19 Z. Kovarik, Z. Radi, H. A. Berman and P. Taylor, *Toxicology*, 2007, **233**, 79.
20 M. Katalini, Z. Kovarik, *Croat. Chem. Acta*. 2012, **85**, 209.
21 (a) R. Cochran, J. Kalisiak, T. Küçükkilinç, Z. Radić, E. Garcia, L. Zhang, K. –Y. Ho, G. Amitai, Z. Kovarik, V. V. Fokin, K. B. Sharpless and P. Taylor, *J. Bio. Chem.*, 2011, **286**, 29718; (b) Z. Kovarik, N. M. Hrvat, M. Katalinić, R. K. Sit, A. Paradyse, S. Žunec, K. Musilek, V. V. Fokin, P. Taylor and Z. Radić, *Chem. Res. Toxicol*., 2015, **28**, 1036; (c) Z. Kovarik, N. Maček, R. K. Sit, Z. Radić, V. V. Fokin, K. B. Sharpless, P.Taylor, *Chemico-Biological Interactions*, 2013, **203**, 77.
22 P. Taylor, Z. Kovarik, E. Reiner and Z. Radi, *Toxicology*, 2007, **233**, 70.
23 Y. P. Pang, T. M. Kollmeyer, F. Hong, J. C. Lee, P. I. Hammond, S. P. Haugabouk and S. Brimijoin, *Chem. Biol.* 2003, **10**, 491.
24 N. Eswar, M. A. Marti-Renom, B. Webb, M. S. Madhusudhan, D. Eramian, M. Shen, U. Pieper and A. Sali, Comparative Protein Structure Modeling With MODELLER. Current Protocols in Bioinformatics, John Wiley & Sons, Inc., Supplement 2006, **15**, 5.6.1.
25 F. Mohamdi, N.G.J. Richards, W.C. Guida, R. Liskamp, M. Lipton, C. Caufield, G. Chang, T. Hendrickson and W.C. Still, *J. Comput. Chem*. 1990, **11**, 440.
26 GROMACS 4.6.3 program package, freely available from the GROMACS website.
27 T. Darden, D. York and L. Pedersen, *J. Chem. Phys.* 1993, **98**, 10089.
28 M. K. Kesharwani, B. Ganguly, A. Das and T. Bandyopadhyay, *Acta. Pharmacol. Sin*. 2010, **31**, 313.
29 R. Lo and B. Ganguly, *Mol. BioSyst.* 2014, **10**, 2368.
30 A. C. Wallace, R. A. Laskowski and J. M. Thornton, *Protein Eng*, 1995, **8**, 127.
31 (*a*) Y. Zhao and D. G. Truhlar, *Acc. Chem. Res.* 2008, **41**, 157; (*b*) W. J. Hehre, L. Radom, P. v. R. Schleyer and J. A. Pople, *Ab Initio Molecular Orbital Theory*, Wiley, New York, 1988.
32 M.J. Frisch, G.W. Trucks, H.B. Schlegel, G.E. Scuseria, M.A. Robb, J.R. Cheeseman, G. Scalmani, V. Barone, B. Mennucci, G.A. Petersson, H. Nakatsuji, M. Caricato, X. Li, H.P. Hratchian, A.F. Izmaylov, J. Bloino, G. Zheng, J.L. Sonnenberg, M. Hada, M. Ehara, K. Toyota, R. Fukuda, J. Hasegawa, M. Ishida, T. Nakajima, Y. Honda, O. Kitao, H. Nakai, T. Vreven, J.A. Montgomery, Jr, J.E. Peralta, F. Ogliaro, M. Bearpark, J.J. Heyd, E. Brothers, K.N. Kudin, V.N. Staroverov, T. Keith, R. Kobayashi, J. Normand, K. Raghavachari, A. Rendell, J.C. Burant, S.S. Iyengar, J. Tomasi, M. Cossi, N. Rega, J.M. Millam, M. Klene, J.E. Knox, J.B. Cross, V. Bakken, C. Adamo, J. Jaramillo, R. Gomperts, R.E. Stratmann, O. Yazyev, A.J. Austin, R. Cammi, C. Pomelli, J.W. Ochterski, R.L. Martin, K. Morokuma, V.G. Zakrzewski, G.A. Voth, P. Salvador, J.J. Dannenberg, S. Dapprich, A.D. Daniels, O. Farkas, J.B. Foresman, J.V. Ortiz, J. Cioslowski, D.J. Fox Gaussian 09, Revision B01, Gaussian, Inc, Wallingford CT 2010.
33 J. Morfill, J. Neumann, K. Blank, U. Steinbach, E. M. Puchner and K. E. Gottschalk, *J Mol Biol* 2008, **381**, 1253.
34 P. E. Marszalek, H. Lu, H. Li, M. Carrion-Vazquez, A. F. Oberhauser and K. Schulten, *Nature* 1999, **402**, 100.
35 B. Heymann and H. Grubmüller, *Phys Rev Lett* 2000, **84**, 6126.
36 C. Chambers, C. Luo, M. Tong, Y. Yang and A. Saxena, *Toxicology in Vitro*, 2015, **29**, 408.
37 C. Luo, C. Chambers, N. Pattabiraman, M. Tong, P. Tipparaju and A. Saxena, *Biochem. Pharmacol*. 2010, **80**, 1427.